Experimental Observation of Localized Optical Excitations in Random Metal-Dielectric Films

S. Grésillon,[1,2] L. Aigouy,[1,2] A. C. Boccara,[1,2] and J. C. Rivoal[2]
[1]*CNRS UPR A0005, 75231 Paris Cedex 05, France*
[2]*Laboratoire d'Optique Physique, ESPCI, Université Pierre et Marie Curie, 75231 Paris Cedex 05, France*

X. Quelin, C. Desmarest, and P. Gadenne
LMOV, Université de Versailles Saint-Quentin, 78035 Versailles, France

V. A. Shubin, A. K. Sarychev, and V. M. Shalaev
Department of Physics, New Mexico State University, Las Cruces, New Mexico 88003
(Received 28 January 1999)

Localization of optical excitations within subwavelength areas of a random metal-dielectric film is observed using near-field scanning optical microscopy. This effect is attributed to Anderson localization of surface plasmon modes in a semicontinuous metal film. The localized modes are seen as giant fluctuations of local electric fields spatially concentrated in "hot" spots, where the fields are much greater than the applied field. The local near-field spectra consisting of strong resonance peaks are detected and shown to depend markedly on the sample site probed. The observed spectral peaks correspond to localized modes of random metal-dielectric films. [S0031-9007(99)09244-3]

PACS numbers: 73.20.Mf, 07.79.Fc

Random metal-dielectric thin films are known to manifest electromagnetic properties that are absent for metal and dielectric components [1]. Such films (also referred to as semicontinuous metal films) can be produced by thermal evaporation or sputtering of metal onto an insulating substrate. In the growing process, coalescence of initially isolated metal grains results in the formation of irregularly shaped fractal clusters of the grains. At the percolation threshold a continuous conducting path of metal appears between the ends of the film (referred, in this case, as to a percolation film).

In this paper, we report direct experimental observation of the localized surface plasmon (SP) modes in metal-dielectric films. The localization is similar to Anderson localization, but it occurs in nanometer-scale areas of a semicontinuous metal film (i.e., well beyond the wavelength limit) and results in the giant enhancement of local fields. We also perform near-field spectroscopy of SP modes and show that the local spectra can differ significantly even for subwavelength distances between the probed sites of the film. Localization of optical excitations in semicontinuous films was first conjectured in our recent paper [2], where it was also supported by numerical simulations. Here we develop more rigorous theoretical arguments for Anderson localization of surface plasmons and, most importantly, provide direct experimental evidence for the localization.

Below we first consider a percolation film for the special case of $-\epsilon_m' = \epsilon_d$, where $\epsilon_m \equiv \epsilon_m' + i\epsilon_m''$ and ϵ_d are the dielectric constants of the metallic and dielectric components. For a $2d$ system, this case corresponds to the SP resonance of individual (noninteracting) metal particles in a dielectric host. We show that the problem of SP resonances maps the Anderson transition problem. Therefore we conclude that the SP modes are localized and find the corresponding local field distribution for $-\epsilon_m' = \epsilon_d$. To calculate the fields in the long-wavelength part of the spectrum, where $|\epsilon_m| \gg \epsilon_d$, we employ the scaling renormalization. For estimates, we use the Drude model with $\epsilon_m = \epsilon_b - (\omega_p/\omega)^2/(1 + i\omega_\tau/\omega)$, where ϵ_b is the interband contribution, ω_p is the plasma frequency, and ω_τ is the plasmon relaxation rate ($\omega_\tau \ll \omega_p$).

When wavelength λ of an incident beam is much larger than the particle size a, we can introduce the potential $\phi(\mathbf{r})$ and the field distribution problem reduces to finding a solution for the equation $\nabla \cdot \{\epsilon(\mathbf{r})[-\nabla\phi(\mathbf{r}) + \mathbf{E}_0]\} = 0$, representing the current conservation law. When discretized on a square lattice, this formula acquires the form of Kirchhoff's equation $H\phi = \mathcal{E}$, where vectors ϕ and $\mathcal{E}$ (proportional to the applied field E_0) are defined in each site of the square lattice. The Kirchhoff equations are characterized by the Hamiltonian H [referred to as the Kirchhoff Hamiltonian (KH)] with off-diagonal elements $H_{ij} = -\epsilon_{ij}$ and diagonal elements $H_{ii} = \sum_j \epsilon_{ij}$, where j refers to the nearest neighbors of i and ϵ_{ij} take values ϵ_m and ϵ_d for metal and dielectric bonds, respectively. In the case $-\epsilon_m' = \epsilon_d$, the values of ϵ_m' and ϵ_d are of the order of unity and different in sign, so that the manifold of the KH eigenmodes contains the modes with the eigenvalues Λ equal (or close) to zero. From the fact that the KH formally maps the Hamiltonian for the Anderson transition problem, with both on- and off-diagonal correlated disorder [3], it follows that its eigenstates are localized within a certain size $\xi_A(\Lambda)$, for the considered $2d$ films. [From the computer simulations of [2], we can deduce that the Anderson localization length $\xi_A(\Lambda)$ is estimated to vary between a and $10a$.] The localized SP modes

 0031-9007/99/82(22)/4520(4)$15.00

with $\Lambda_n \to 0$ are strongly excited by the applied field and seen as giant field fluctuations.

For further analysis it is convenient to normalize the permittivities as $\epsilon_m = -1 + i\kappa$ and $\epsilon_d = 1$, where $\kappa = \epsilon_m''/|\epsilon_m'| \ll 1$. The Kirchhoff equations can be written then as $(H' + i\kappa H'')\phi = \mathcal{E}$, where H' and H'' are both Hermitian, and $\kappa H'' \ll 1$ represents losses in the system. We express now the potential ϕ in terms of the eigenfunctions ψ_n of H' as $\phi = \sum_n A_n\psi_n$. We then obtain $(i\kappa b + \Lambda_n)A_n + i\kappa\sum_{m\neq n}(\psi_n|H''|\psi_m)A_m = \mathcal{E}_n$, where $b = (\psi_n|H''|\psi_n) \sim 1$, and $\mathcal{E}_n = (\psi_n \mid \mathcal{E}) \sim E_0 a$ is the projection of the external field on the eigenstate ψ_n. Provided that ψ_n are localized, the sum in the above expression converges and may be treated as a small perturbation. In the zeroth approximation, $A_n = \mathcal{E}_n/(\Lambda_n + i\kappa b)$. The first correction to A_n is equal to $A_n' = -i\kappa\sum_{m\neq n} \times (\psi_n|H''|\psi_m)\mathcal{E}_m/(\Lambda_m + i\kappa b)$. For $\kappa \to 0$, the most important modes with $|\Lambda_m| \leq \kappa$ have the surface density $a^{-2}\kappa \to 0$. Therefore A_n' is exponentially small, $A_n' \sim \exp\{-a/[\xi_A(0)\sqrt{\kappa}]\}$, and can be neglected when $\kappa \ll (a/\xi_A)^2$ (we set $\xi_A(0) \equiv \xi_A$). Then, the local potential is $\phi(r) = \sum_n \mathcal{E}_n\psi_n(r)/(\Lambda_n + i\kappa b)$; it strongly fluctuates, and the average field intensity can be estimated as

$$\langle|E|^2\rangle \approx \langle|\nabla\phi(\mathbf{r})|^2\rangle = \left\langle \sum_{n,m} \frac{\mathcal{E}_n\mathcal{E}_m^*[\nabla\psi_n(\mathbf{r})\cdot\nabla\psi_m^*(\mathbf{r})]}{(\Lambda_n + i\kappa)(\Lambda_m - i\kappa)} \right\rangle, \tag{1}$$

where, for simplicity, we set $b = 1$. For a macroscopically homogeneous random film, the spatial locations of ψ_n do not correlate with the value of Λ_n, so that we can independently average the numerator in Eq. (1). Taking into account that $\langle\nabla\psi_n(\mathbf{r})\rangle = 0$ and $\langle|\nabla\psi_n(\mathbf{r})|^2\rangle \propto \xi_A^{-2}(\Lambda_n)$ for a localized state, we obtain

$$\langle|E|^2\rangle \approx \sum_n \frac{|\mathcal{E}_n|^2\langle|\nabla\psi_n(\mathbf{r})|^2\rangle}{\Lambda_n^2 + \kappa^2} \sim E_0^2\int \frac{\rho(\Lambda)[a/\xi_A(\Lambda)]^2}{\Lambda^2 + \kappa^2}\, d\Lambda, \tag{2}$$

where $\rho(\Lambda) = (a^2/S)\sum_n \delta(\Lambda - \Lambda_n)$ is the dimensionless density of states for H' (S is the total area). Since all values in H' are of the order of unity $\rho(0) \sim 1$, and $\langle|E|^2\rangle$ at $-\epsilon_m' = \epsilon_d = 1$ is estimated as $\langle|E|^2\rangle \sim E_0^2(a/\xi_A)^2\kappa^{-1} \gg E_0^2$, provided $\kappa \ll (a/\xi_A)^2$. Thus the field distribution, in this case, can be described as a set of the KH eigenfunctions localized within ξ_A, with the field peaks having the amplitudes $E_m \sim E_0\kappa^{-1}(a/\xi_A)^2$, which are separated in distance by the field correlation length $\xi_e \sim a/\sqrt{\kappa} \gg \xi_A$.

Now we turn to the important case of the "high contrast," with $|\epsilon_m| \gg \epsilon_d$, that corresponds to the long-wavelength part of the spectrum. From basic principles of Anderson localization [3], it is clear that a higher contrast favors localization. To obtained the field distribution, we renormalize the system to the above case of $-\epsilon_m' = \epsilon_d$ by considering square elements of the size $l_r = a\sqrt{|\epsilon_m|/\epsilon_d}$ as new elements [2]. Using the known scaling dependences for a percolation film $\epsilon_m(l) \sim (l/a)^{-t/\nu}\epsilon_m$ and $\epsilon_d(l) \sim (l/a)^{s/\nu}\epsilon_d$ [1], we obtain that $-\epsilon_m(l_r) = \epsilon_d(l_r)$, for the renormalized elements of the resonant size l_r. (For $d = 2$, in the formulas above, $t \approx s \approx \nu \approx 4/3$ are the percolation critical exponents for conductivity, dielectric constant, and percolation correlation length.) In the renormalized system, the above estimate for E_m holds. Since the electric field and eigenfunctions scale as l_r we conclude that in the original system $\langle|E|^2\rangle \sim E_0^2\kappa^{-1}(a/\xi_A)^2 l_r/a$. The field peaks are estimated as $E_m \sim E_0(a/\xi_A)^2|\epsilon_m|^{3/2}/(\epsilon_d^{1/2}\epsilon_m'')$ and the light-induced eigenmodes are separated, on average, by the distance $\xi_e \sim l_r/\sqrt{\kappa} \sim a|\epsilon_m|/\sqrt{\epsilon_m''\epsilon_d}$. For a Drude metal at $\omega \ll \omega_p$, the local field peaks are $E_m/E_0 \sim \epsilon_d^{-1/2}(a/\xi_A)^2 \times (\omega_p/\omega_\tau)$, and the distance between the excited modes is $\xi_e \sim a\omega_p/\sqrt{\epsilon_d\omega\omega_\tau}$.

The following pattern of the local field distribution emerges from the above scaling theory. The largest local fields of the amplitude E_m result from excitation of the resonant clusters of the size l_r. With increasing the wavelength (and thus the contrast $|\epsilon_m|/\epsilon_d$), both the resonant size l_r and the distance ξ_e between the resonating modes increase. Since at the percolation threshold the system is scale invariant, for any ω of the applied field, there are always resonating metal clusters that have the appropriate size $l_r(\omega) \sim a(\omega_p/\omega)$.

We performed imaging and spectroscopy of localized optical excitations in gold-on-glass percolation films, using scanning near-field optical microscopy (SNOM). The used SNOM probe is an apertureless tip made of a tungsten wire etched by electrochemical erosion [4]. The radius of curvature of the tip measured by scanning electron microscopy is about 10 nm, which provides the very high spatial resolution needed to image the localized optical modes. The tip is set above a sample which is attached to an (x, y) horizontal piezoelectric stage. The tip is the bent end of the tungsten wire used as a cantilever connected to a twin-piezoelectric transducer that can excite it perpendicularly to the sample surface. The frequency of vibrations (~5 kHz) is close to the resonant frequency of the cantilever and its amplitude is about 100 nm. In the tapping mode the tip vibrates above the sample as in an atomic force microscope (AFM). Detection of the vibration amplitude is made by a transverse laser diode probe beam focused at the lever arm. A feedback system, including a piezoelectric translator attached to the twin-piezoelectric transducer (needed for the tip vibrations), keeps constant the vibration amplitude during the sample scanning. The detection of the feedback voltage applied to the piezoelectric translator gives a topographical image of the surface, i.e., the AFM signal that can be taken simultaneously with the SNOM signal. A first microscope objective focuses the light of tunable cw Ti:sapphire laser on the bottom surface of the sample. The signal collection is axially symmetric

above the sample and it is made by a second microscope objective. The transmitted light passing through the microscope is then sent to a photomultiplier.

The tip vibration modulates the near-zone field on a sample surface, and lock-in detection of the collected light at the tip's vibrational frequency allows one to detect the locally modulated field [4]. We note that the detected signal in such a SNOM technique is proportional to the amplitude of the modulated local field rather than its intensity. In order to relate our results to other near-field measurements (where the local intensity is typically measured) the results shown below are squared to display the intensity of the detected signal.

For the visible and near-IR parts of the spectrum, the tungsten tip ($n \approx 3.5 + 2.8i$) does not have any resonances so that its polarizability is much less than the polarizability of the resonance-enhanced plasmon oscillations of the film. Because of this, perturbations in the field distribution introduced by the tip are relatively small. Our calculations of the tip perturbations, when it is modeled as a polarizable sphere, support this conclusion [4].

Samples of semicontinuous metal films were prepared by depositing gold thin films on a glass substrate at room temperature under ultrahigh vacuum (10^{-9} Torr). In order to determine a closeness to the percolation threshold, the resistivity and the deposited mass thickness were measured all along the film deposition. Optical reflection and transmission of the samples were also determined out of the vacuum chamber and compared with the well-known optical properties of percolation samples [5]. Transmission electron microscopy was performed afterwards by depositing the same film on a Cu grid covered by a very thin SiO_2 layer.

In Figs. 1a and 1b, we show experimental and calculated near-field images at the surface of a percolation gold-glass film, for different wavelengths (experimental and simulated samples are, on average, similar but different locally; the reference point for intensity is set at the mean value). In experimental SNOM images, resolution of one pixel is 10 nm, which is near the best resolution that can be achieved by SNOM. Note that optical excitations are strongly localized in both horizontal and vertical directions. Our estimations show that the signal becomes negligible at the tip-sample separation $\sim$10 nm. This means that in the tapping mode with the oscillation amplitude 100 nm, the detected average signal is strongly decreased, by factor $1/10$ or even $1/100$. To somehow approximate this effect and a finite size of the tip, we choose in our simulations the tip-sample separation 10 nm and average the collected signal over the area 50×50 nm^2.

The observed near-field images are in qualitative agreement with theoretical predictions and numerical simulations. The optical excitations of a percolation film are localized in $\sim$100-nm-size areas, significantly smaller than λ. A small number of peaks is observed in the probed area and thus no reliable statistical analysis can be made with the available data. Nevertheless, the tendency for the field amplitudes to increase with the wavelength, as our theory predicts, can be easily traced in Fig. 1a, despite the small change in λ (less than 10%).

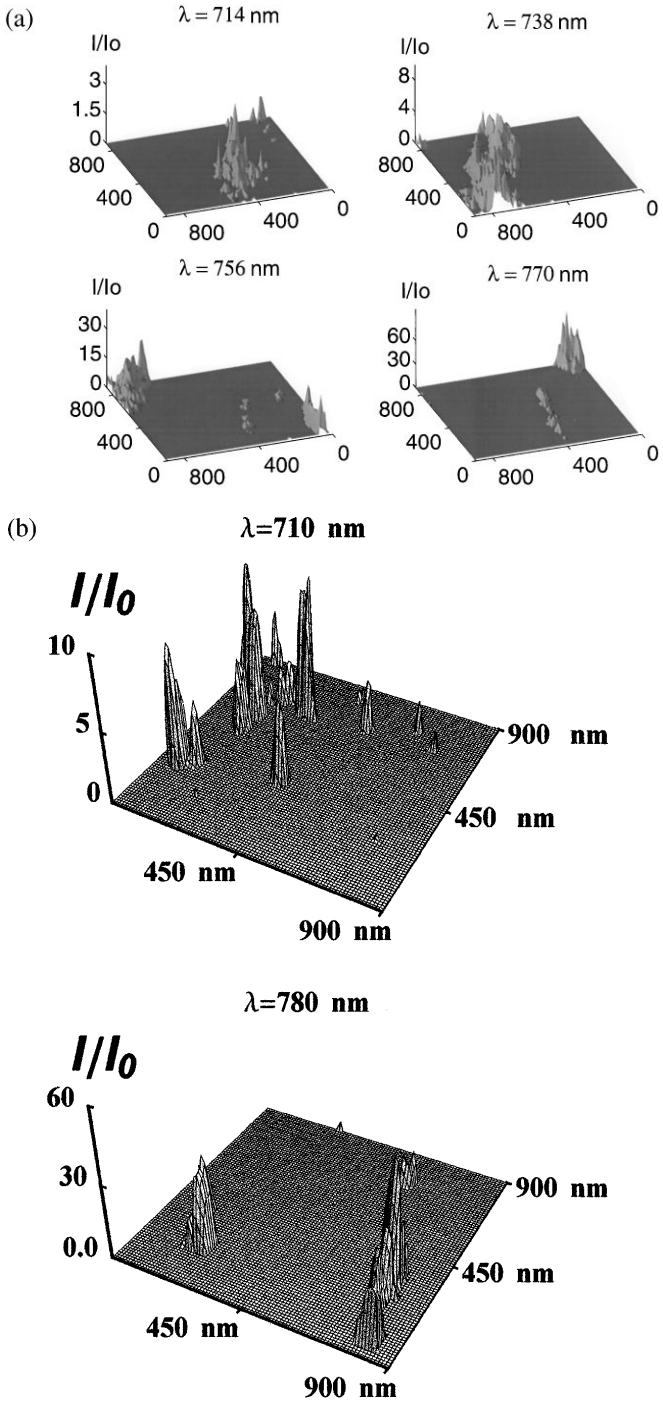

FIG. 1. Experimental (a) (nm units are used for the x, y coordinates) and calculated (b) SNOM images of the localized optical excitations in a percolation gold-on-glass film for different wavelengths λ.

For the SNOM detection, the experimentally observed and simulated enhancement of the local field intensity is

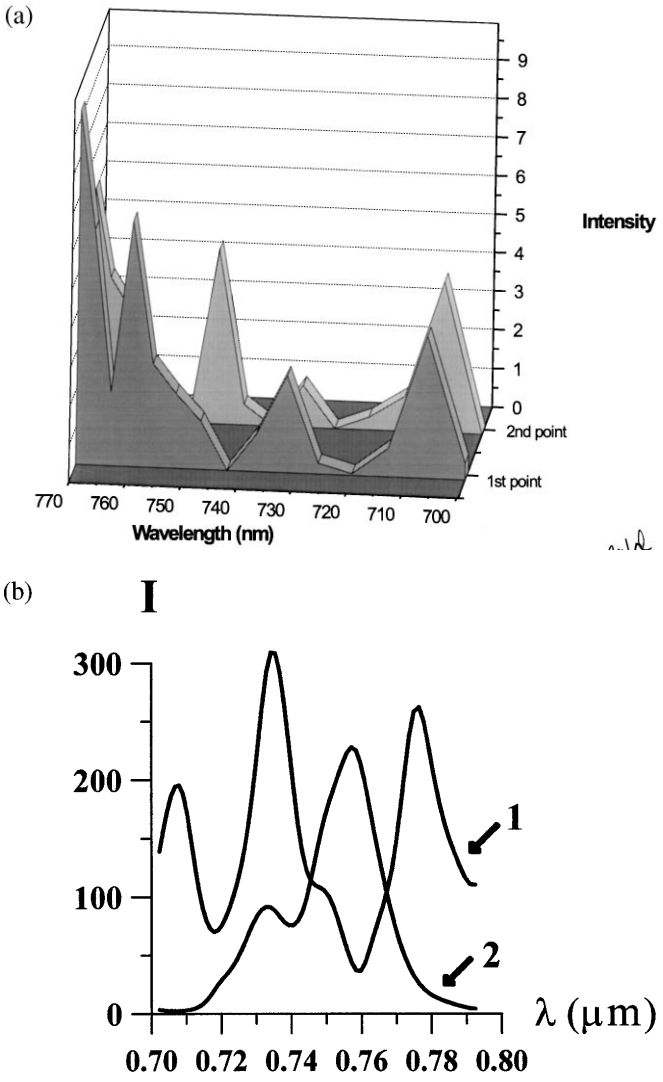

FIG. 2. Experimental (a) and calculated (b) near-field spectra at different spatial locations (100 nm apart) of the film. (Arbitrary intensity units are used.)

10 to 10^2. However, according to our calculations (not shown), the local field intensity right on the surface of the film (which can be probed, for example, by surface-adsorbed molecules) is much larger than the averaged signal detected by the SNOM tip, by roughly 2 orders of magnitude. Note that both observed and calculated near-field images are λ dependent: Even as small a change of wavelength as $\Delta\lambda \sim \lambda/50$ results in dramatically different field distributions.

We also performed the near-field spectroscopy of percolation films, by parking a SNOM tip at different points of the surface and varying the wavelength. This local nano-spectroscopy allows one to determine the local resonances of nm-size areas right underneath the tip; the nanostructures at different points resonate at different λ, leading to different local near-field spectra. The spectra characterize the λ dependence of the field hot spots associated with the localized SP modes.

In Figs. 2a and 2b we show the measured and calculated near-field spectra taken at different points of the film. Again, there is qualitative agreement between theory and experiment. The spectra consist of several peaks $\sim$10 nm in width, and they depend markedly on spatial location of the point where the near-field tip is parked. Even as small a shift in space as 100 nm results in different spectra, which is strong evidence of the SP-mode localization. For continuous metal (or dielectric) films, neither sub-λ hot spots nor their local spectra can be observed, because, in this case, optical excitations are delocalized.

In conclusion, the near-field imaging and spectroscopy of random metal-dielectric films near percolation suggest localization of optical excitations in small nm-scale hot spots. The observed patterns of the localized modes and their spectral dependences are in agreement with theoretical predictions and numerical simulations. The hot spots of a percolation film represent very large local fields (fluctuations); spatial positions of the spots strongly depend on the light frequency. Near-field spectra observed and calculated at various points of the surface consist of several spectral resonances whose spectral locations depend on the probed site of the sample. All of these features are only observable in the near zone. In the far zone, one observes images and spectra in which the hot spots and the spectral resonances are averaged out. The local field enhancement is large, which is especially important for nonlinear processes of the nth order proportional to the enhanced local fields to the nth power. This opens a fascinating possibility for *nonlinear* near-field spectroscopy of single nanoparticles and molecules.

This work was supported in part by NSF under Grant No. DMR-9810183, PRF under Grant No. 32319-AC5, ARO under Grant No. DAAG55-98-1-0425, and RFFI Grant No. 98-02-17628. Useful discussions with S. Bozhevolnyi are appreciated.

[1] D. J. Bergman and D. Stroud, Solid State Phys. **46**, 147 (1992); D. Stauffer and A. Aharony, *Introduction to Percolation Theory* (Taylor & Francis, London, 1994).

[2] V. M. Shalaev and A. K. Sarychev, Phys. Rev. B **57**, 13 265 (1998); F. Brouers *et al.*, Phys. Rev. B **55**, 13 234 (1997); *ibid.* **58**, 15 897 (1998).

[3] B. Kramer and A. MacKinnon, Rep. Prog. Phys. **56**, 1469 (1993); K. B. Efetov, *Supersymmetry in Disorder and Chaos* (Cambridge University Press, Cambridge, England, 1997).

[4] R. Bachelot *et al.*, Appl. Opt. **36**, 2160 (1997); P. Gleyzes *et al.*, Appl. Phys. Lett. **58**, 2989 (1991); A. Lahrech *et al.*, Opt. Lett. **21**, 1315 (1996).

[5] P. Gadenne *et al.*, J. Appl. Phys. **66**, 3019 (1989); Y. Yagil *et al.*, Phys. Rev. B **46**, 2503 (1992).